Description and explanation of electromagnetic behaviors in artificial metamaterials based on effective medium theory

Ruopeng Liu,[1,2] Tie Jun Cui,[1,*] Da Huang,[1] Bo Zhao,[1] and David R. Smith[2,†]

[1]*Center for Computational Electromagnetics and the State Key Laboratory of Millimeter Waves, Department of Radio Engineering, Southeast University, Nanjing 210096, People's Republic of China*

[2]*Department of Electrical and Computer Engineering, Duke University, Box 90291, Durham, North Carolina 27708, USA*

(Received 11 April 2007; published 23 August 2007)

We present a general theory of effective media to set up the relationship between the particle responses and the macroscopic system behaviors for artificial metamaterials composed of periodic resonant structures. By treating the unit cell of the periodic structure as a particle, we define the average permittivity and permeability for different unit structures and derive a general form of discrete Maxwell's equations on the macroscale, from which we obtain different wave modes in metamaterials including the propagation mode, pure plasma mode, and resonant crystal band-gap mode. We explain unfamiliar behaviors of metamaterials from the numerical *S* parameter retrieval approach. The excellent agreement between theoretical predictions and retrieval results indicates that the defined model and method of analysis fit the physical structures very well. Thereafter, we propose a more advanced form of the fitting formulas for the effective electromagnetic parameters of metamaterials.

DOI: 10.1103/PhysRevE.76.026606 PACS number(s): 41.20.Jb, 84.40.Az, 78.20.Ci, 42.25.Bs

I. INTRODUCTION

Artificially structured electromagnetic metamaterials have received considerable attention over the past several years due to their ability to exhibit a large range of electromagnetic responses not readily found in naturally occurring materials and composites [1]. Since the demonstration of an artificial medium with negative refractive index in 2001 [2], metamaterial designs have increased in complexity and sophistication, to the point that precisely controlled gradients in both permittivity and permeability can be introduced to form advanced lenses and optics [3,4], or even invisibility cloaks [5,6].

While not a necessary requirement, periodicity is a feature typically found in metamaterials, which are usually based on repeated unit cells containing one or more conducting resonators. Unlike photonic crystals, though, the unit cell size in metamaterials is much smaller than the free-space wavelength, so that the otherwise inhomogeneous structure can be homogenized from an electromagnetic point of view. The procedure of homogenization enables effective constitutive parameters—the electric permittivity and the magnetic permeability, for example—to be defined and used to characterize the composite.

Although the use of effective constitutive parameters has proved successful in describing and predicting the properties of waves propagating in metamaterials, the retrieved parameters nevertheless display anomalous and often nonintuitive behavior. For example, it was found from scattering (*S*) parameter simulations that when either the retrieved permittivity or permeability possesses a resonance form, there is an accompanying antiresonance in the nonresonant parameter over the same frequency range, with the sign of the imaginary part of the antiresonant parameter opposite to that of the resonant parameter [7]. Considerable discussion has ensued over the applicability of retrieval methods and even the validity of effective constitutive parameters in general for metamaterial structures [8].

The unusual form of the constitutive parameters obtained from retrieval methods has recently been analyzed with increasing rigor by numerous researchers [8–13]. The consensus that has emerged is that the periodicity associated with most reported metamaterials, usually a factor of ten smaller than the free-space wavelength, plays a significant role in the metamaterial properties. As a result, the closed form expressions obtained by researchers in the static and quasistatic limits for the constitutive parameters [14–17], which is typically in the form of a Drude or Drude-Lorentz model, must be modified to include the effects of spatial dispersion.

To date, there has not been a theoretical approach that connects well the simple medium dispersion models to the actual retrieved parameters of metamaterial structures. As a result, the detailed design of metamaterials has relied entirely on numerical approaches that one first solves Maxwell's equations for a structure and then performs a numerical retrieval to obtain the effective constitutive parameters. Well-known effective medium approaches can be used to form an initial metamaterial design and develop a working intuition, but do not predict the ultimate frequency-dependent form that the actual parameters usually take. Our aim here is to present a dispersion form linking actual particle response and periodic system behaviors that provides a simplified, yet accurate, description of metamaterials and is also entirely consistent with and gives very clear physics explanations of previous numerical extraction approaches.

Recently, a rigorous approach to the numerical retrieval of the constitutive parameters was presented, in which field averages over the metamaterial unit cell were used to determine the macroscopic fields [8]. A similar approach has also been applied to the transmission-line formulations of metamateri-

*tjcui@seu.edu.cn
†drsmith@ee.duke.edu

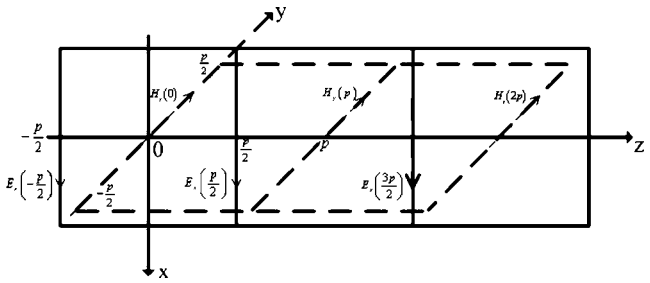

FIG. 1. Metamaterial composed of periodic particles, where a TEM wave is incident along the z direction.

als [18–20]. This process results in a discrete form of Maxwell's equations, in which the metamaterial unit cell is replaced by an effective medium. The discrete set of equations, though, implies that the fields are effectively sampled on a finite grid, so that spatial dispersion is inherent in the formulation. Although ultimately a numerical implementation, the method presented in [8] forms a useful starting point for the present discussion.

In this paper, we build up a metamaterial system by dividing two different levels, which correspond to a particle response in terms of average permittivity and permeability and a system behavior in terms of effective permittivity and permeability, respectively. The particle response actually has been well studied by static or quasistatic field analysis [13–15]. Thus, the key point becomes to set up a link between the particle response and the system behavior.

II. AVERAGE PERMITTIVITY AND PERMEABILITY

We start our analysis here from the integral form of Maxwell's equations. Consider an artificial material composed of arbitrary elements repeated periodically, as shown in Fig. 1, in which the periodicities in the x, y, and z directions are equal to p. An incident electromagnetic wave with transverse electric and magnetic (TEM) fields propagates along the z direction. The electric field is x polarized, and the magnetic field is y polarized. Periodic boundary conditions are assumed in the x and y directions. Applying Faraday's theorem to the first cell in the x-z plane for the electric field, we obtain

$$\int_{-p/2}^{p/2} E(x,0,p/2)dx - \int_{-p/2}^{p/2} E(x,0,-p/2)dx = i\omega \int_{S_{xz}} \mu_a H(x,0,z)ds, \tag{1}$$

in which μ_a is the permeability of the background medium. As in Ref. [8], we define the averaged electric field $\bar{E}_x$ and the magnetic field $\bar{H}_y$ by line integrals,

$$\bar{E}_x(z) = \frac{1}{p}\int_{-p/2}^{+p/2} E(x,0,z)dx, \tag{2}$$

$$\bar{H}_y(z) = \frac{1}{p}\int_{-p/2}^{+p/2} H(0,y,z)dy. \tag{3}$$

From inspection of Eq. (1), we see that the averaged magnetic field $\bar{B}_x$ emerges naturally as a surface integral, so that the average permeability $\bar{\mu}$ has the form [9]

$$\bar{\mu} = \frac{1}{p^2\bar{H}_y(0)}\int_{-p/2}^{+p/2}\int_{-p/2}^{+p/2} \mu_a H(x,0,z)dx\,dz. \tag{4}$$

Equation (1) may thus be written as

$$\bar{E}_x(p/2) - \bar{E}_x(-p/2) = i\omega\bar{\mu}p\bar{H}_y(0). \tag{5}$$

The above equation can be extended to any cell n along the z direction:

$$\bar{E}_x[(n+1/2)p] - \bar{E}_x[(n-1/2)p] = i\omega\bar{\mu}p\bar{H}_y(np). \tag{6}$$

Similarly, the other Maxwell equation in the integral form can be simplified to

$$\bar{H}_y[(n+1)p] - \bar{H}_y[np] = i\omega\bar{\varepsilon}p\bar{E}_x[(n+1/2)p] \tag{7}$$

after introducing the average permittivity

$$\bar{\varepsilon} = \frac{1}{p^2\bar{E}_x(p/2)}\int_{-p/2}^{+p/2}\int_{-p/2}^{+p/2} \varepsilon_a E(0,y,z)dy\,dz, \tag{8}$$

in which ε_a is the permittivity of the background medium. Equations (6) and (7) together represent a discrete set of Maxwell's equations (DME) that can be solved for TEM waves.

Based on Eqs. (4) and (8), the average constitutive parameters are defined in terms of field averages, which is consistent with the previous work on the homogenization of metamaterials [9]. The average parameters represent the local field responses by structures with finite dimension, from which we can group the actual unit structure as a particle. Hence we can separate the whole model into a particle level to obtain average parameters and a system level to obtain effective parameters in terms of average parameters.

III. AVERAGE DISPERSION EQUATION AND AVERAGE PARTICLE-WAVE IMPEDANCE

In order that DME represent an infinite periodic structure, we apply the Bloch boundary conditions: $\bar{E}_x[(n+1/2)p] = \bar{E}_x[p/2]e^{i(n\theta+\theta/2)}$ and $\bar{H}_y[(np)] = \bar{H}_y[0]e^{in\theta}$, in which θ is the phase advance across one cell. Substituting the boundary conditions into the DME, we obtain the dispersion equation

$$\sin(\theta/2) = S_d\omega p\sqrt{\bar{\mu}\bar{\varepsilon}}/2, \tag{9}$$

where $S_d=1$ if the wave is propagating in a material where $\bar{\varepsilon}$ and $\bar{\mu}$ are both positive, and $S_d=-1$ if the wave is propagating in a material where $\bar{\varepsilon}$ and $\bar{\mu}$ are both negative. Equation (9) can be solved, yielding

$$\theta = 2\arg(A) - 2i\ln(|A|), \tag{10}$$

in which $A = iS_d\omega p\sqrt{\bar{\mu}\bar{\varepsilon}}/2 + \sqrt{1-\omega^2p^2\bar{\mu}\bar{\varepsilon}/4}$. We remark that the second term of A is real when $\omega^2p^2\bar{\mu}\bar{\varepsilon} < 4$ but imaginary when $\omega^2p^2\bar{\mu}\bar{\varepsilon} > 4$. In the latter case, the square root is de-

fined as $-iS_d\sqrt{\omega^2 p^2 \bar{\mu}\bar{\varepsilon}/4-1}$ to make $|A|<1$ the requirement for passive media.

Equation (9) shows that the phase advance is related not only to the average constitutive parameters, but also to the periodicity p. In the other words, the metamaterial exhibits both frequency and spatial dispersions. The latter cannot be eliminated unless the periodicity p goes to zero, which corresponds to the case of a homogeneous medium. To obtain a complete description of wave propagation in a medium, it is necessary also to determine the wave impedance of the medium. Unless the periodicity is zero, however, the wave impedance varies across the unit cell according to its definition: $\eta(z)=\bar{E}_x(z)/\bar{H}_y(z)$. The general expression for the impedance will be complicated in form, depending on the nature and the geometry of the specific metamaterial elements within the unit cell. However, under certain conditions that occur commonly in metamaterial structures, a relatively simple form of the impedance can be obtained. A rough justification can be obtained by assuming the field by applying the Bloch boundary conditions to Eqs. (6) and (7) as was done to find the phase advance.

Part of the difficulty in obtaining a wave-impedance expression is that the average electric and magnetic fields for the effective finite-difference Maxwell's equations are defined on the edges of lattices that are offset from each other, whereas the definition of impedance requires a ratio of electric and magnetic fields at the same point. Since metamaterials are usually composed of strong magnetic or electric resonant subwavelength structures, the electric or magnetic field can be approximately modeled to be phase uniform in the unit cell of electric or magnetic resonators. Thus, the field at the edge of unit cell can be estimated approximately using an interpolation of fields in two nearest adjacent lattices. In this way, we arrive at two possible definitions of the impedance; one is obtained by averaging the magnetic field:

$$\eta(np+p/2)=\bar{E}_x(np+p/2)/\bar{H}_y(np+p/2)$$
$$=\frac{2\bar{E}_x(np+p/2)}{\bar{H}_y(np)+\bar{H}_y(np+p)}=\sqrt{\frac{\bar{\mu}}{\bar{\varepsilon}}}\frac{1}{\cos(\theta/2)}, \tag{11}$$

while the other is obtained by averaging the electric field:

$$\eta(np)=\bar{E}_x(np)/\bar{H}_y(np)=\frac{\bar{E}_x(np-p/2)+\bar{E}_x(np+p/2)}{2\bar{H}_y(np)}$$
$$=\sqrt{\frac{\bar{\mu}}{\bar{\varepsilon}}}\cos(\theta/2). \tag{12}$$

The impedance as found in Eqs. (11) and (12) periodically varies along the propagation direction. Whether Eq. (11) and (12) should be used depends on the relative position of the boundary for periodic structures, where the phase matching is conducted in calculation. For magnetic resonators, Eq. (11) will be approximately correct, in which the magnetic field is nearly uniform within one unit cell. Likewise, for electric resonators, Eq. (12) will be approximately correct since the electric field is nearly uniform within one unit cell. The two equations can be combined together to yield a general form

$$\eta=\sqrt{\frac{\bar{\mu}}{\bar{\varepsilon}}}(\cos\theta/2)^{S_b} \tag{13}$$

for the wave impedance. Here, $S_b=1$ is for electric resonators while $S_b=-1$ for magnetic resonators.

IV. GENERAL SOLUTIONS OF EFFECTIVE MEDIA

With the spatial dispersion relation (10) and the spatial wave impedance (13), we can now obtain a compact analytic solution for the constitutive parameters of a metamaterial. Denoting the effective permittivity and permeability as ε_{eff} and μ_{eff}, then the phase shift θ and wave impedance η can be expressed in terms of ε_{eff} and μ_{eff} as $\theta=\omega p\sqrt{\mu_{\text{eff}}\varepsilon_{\text{eff}}}$ and $\eta=\sqrt{\mu_{\text{eff}}/\varepsilon_{\text{eff}}}$. Considering Eqs. (10) and (13), we obtain the general solution for the effective permittivity and permeability as

$$\varepsilon_{\text{eff}}=\bar{\varepsilon}\frac{(\theta/2)}{\sin(\theta/2)}[\cos(\theta/2)]^{-S_b}, \tag{14}$$

$$\mu_{\text{eff}}=\bar{\mu}\frac{(\theta/2)}{\sin(\theta/2)}[\cos(\theta/2)]^{S_b}. \tag{15}$$

Equations (14) and (15) provide a useful approximate solution for electrically or magnetically resonant metamaterials, setting up the relationship between the particle response and the system behavior, as will become clear from comparisons with numerical simulations. Furthermore, in the limit that the metamaterial approaches a homogenized medium (i.e., the wavelength within the medium becomes large in terms of the unit cell size), the solutions are seen to be trivially valid, with the effective constitutive parameters reducing to the background constitutive parameters ($\varepsilon_{\text{eff}}=\varepsilon_a$ and $\mu_{\text{eff}}=\mu_a$).

Next we discuss the general solution in three cases.

A. Propagation modes

In the absence of losses, when $0<\bar{\mu}\bar{\varepsilon}<4/(\omega p)^2$, we see from Eq. (9) that θ is real and thus the corresponding modes are propagating. The effective constitutive parameters predicted by Eqs. (14) and (15) provide useful insight as to the character of the propagating modes. We point out two interesting aspects that have led to anomalous frequency-dependent behavior observed in prior numerical work [12]. First, the wave impedance approaches zero for an electric resonator or infinity for a magnetic resonator when $\theta=\pi$ or $-\pi$. This behavior implies that when either $\bar{\epsilon}$ or $\bar{\mu}$ take large values, then $\bar{\mu}$ or $\bar{\epsilon}$ will take accordingly small values. The medium as a whole in these cases can be viewed as a spatial resonator.

Another interesting phenomenon is that, for lossy media, $\cos(\theta/2)$ becomes a complex number. From Eqs. (14) and (15), we see that one of the constitutive parameters will acquire a negative imaginary part [i.e., negative loss assuming an $\exp(-i\omega t)$ time dependence]. For low-loss media, this "negative loss" is relatively weak, but exists nonetheless be-

cause of the nature of spatial wave impedance. We see that this seemingly unphysical behavior vanishes when p is extremely small or the resonance is weak; in this case, the solution reduces to the usual case of a lossy homogeneous medium.

B. Pure plasma modes

When the average permittivity and permeability satisfy $\bar{\mu}\bar{\varepsilon}<0$, only evanescent waves exist in the metamaterial based on Eq. (9). We see that

$$\varepsilon_{\text{eff}} = \bar{\varepsilon}\frac{(\theta_I/2)}{\sinh(\theta_I/2)}[\cosh(\theta_I/2)]^{-S_b}, \tag{16}$$

$$\mu_{\text{eff}} = \bar{\mu}\frac{(\theta_I/2)}{\sinh(\theta_I/2)}[\cosh(\theta_I/2)]^{S_b}, \tag{17}$$

in which $\theta_I = 2\ln(u+\sqrt{1+u^2})$ with $u=\omega p\sqrt{|\bar{\mu}\bar{\varepsilon}|}/2$. Here, $S_d=1$ has been chosen in this case to make the effective medium passive.

C. Resonant crystal band-gap modes

When the average permittivity and permeability satisfy $\bar{\mu}\bar{\varepsilon}>4/(\omega p)^2$, then Eq. (9) shows that θ will be a complex number, which corresponds to a resonant crystal band-gap mode. The resonant crystal band gap results from the periodicity inherent in the metamaterial combined with the large effective constitutive parameters associated with the resonant metamaterial elements. The resonant crystal band-gap phenomenon is a unique feature of resonant metamaterials, which lie conceptually between photonic crystals and homogenized materials. The phase advance in this regime is given by

$$\theta = S_d\pi + i\theta_I, \tag{18}$$

in which S_d is the dispersion sign defined earlier, corresponding to the left- or right-handed average parameters, and $\theta_I = 2\ln(u+\sqrt{1+u^2})$. Thus the effective permittivity and permeability are expressed as

$$\varepsilon_{\text{eff}} = -S_b\bar{\varepsilon}\frac{\theta_I - i\pi}{\cosh(\theta_I/2)}[\sinh(\theta_I/2)]^{-S_b}, \tag{19}$$

$$\mu_{\text{eff}} = S_b\bar{\mu}\frac{\theta_I - i\pi}{\cosh(\theta_I/2)}[\sinh(\theta_I/2)]^{S_b}. \tag{20}$$

From Eqs. (19) and (20), we observe three important features. First, only evanescent waves are supported in the crystal band-gap regime. Second, the phase shifts by ±180° from one cell to adjacent cells, while the sign of the phase depends on whether the average parameters are both positive or both negative. Finally, the imaginary parts in the effective permittivity and permeability appear in conjugate forms. In other words, the *negative* loss always exists in one of the constitutive parameters, which compensates the *positive* loss in the other parameter to generate an overall lossless behavior.

We see also from Eqs. (19) and (20) that there are two distinct types of crystal band-gap metamaterials: electric, in which the real part of the permittivity is negative, and magnetic, in which the real part of the permeability is negative. The two types are related to whether the metamaterial is composed of electric or magnetic resonators, which is manifest in the sign of S_b in the wave impedance and the sign of the average parameters. The two types of photonic band-gap modes have been confirmed in numerical and experimental studies of evanescent wave amplification by cascaded periodic circuit structures [18]. The modes associated with crystal band-gap metamaterials have a distinct character as compared with conventional photonic crystal structures. In photonic crystals, the periodicity of the index generates the band-gap region due to Bragg reflection. In metamaterials, however, each unit possesses a strong resonance in addition to the periodicity that combine together to introduce spatial dispersions in both the index (phase advance) and the wave impedance.

V. APPLICATIONS AND DISCUSSIONS

In order to validate the analytic theory, we consider three typical metamaterial structures for analysis: the split-ring resonator (SRR), which possesses a strong magnetic resonance [15]; the electric-*LC* (ELC) resonator which has strong electric resonance [16]; and the SRR and wire structure, which is also known as a negative index material. This latter structure possesses both electric and magnetic resonances, but the electric resonance occurs at zero frequency and thus the composite structure appears as a magnetic resonator when Eq. (13) is applied [7]. Since the SRR and SRR-wire media are magnetic-response structures, $S_b=-1$ must be chosen. Similarly, since the ELC is an electric-response structure, we must choose $S_b=1$.

The average and effective constitutive parameters have often been used as an approximate description of metamaterials in previous research, where Drude-Lorentz and similar models have been applied. Yet it is well known that there are significant deviations from these ideal forms when numerical retrievals are performed on simulated or measured data. In fact, the Drude-Lorentz models are accurate, causal descriptions of metamaterials in the limit that spatial dispersion is not a factor (i.e., electro- or magnetostatic limits). In the presence of periodicity, though, the ideal forms are modified in the manner described above. For example, the SRR structure shown in Fig. 2(a) possesses an average permeability in the absence of spatial dispersion of the form

$$\bar{\mu}_{\text{SRR}} = \mu_a[1 - Ff^2/(f^2 - f_0^2 + i\gamma f)], \tag{21}$$

in which f_0 is the magnetic resonant frequency, and γ is the loss factor. The SRR usually does not exhibit a strongly dispersive permittivity, so we take for the average permittivity $\bar{\epsilon}_{\text{SRR}}=\epsilon_a\sin(v)/v$ as homogeneous model for background medium based on Eq. (8), in which $v=\omega p\sqrt{\varepsilon_a\mu_a}/2$. For the ELC resonator shown in Fig. 2(b), the average permittivity is of the form

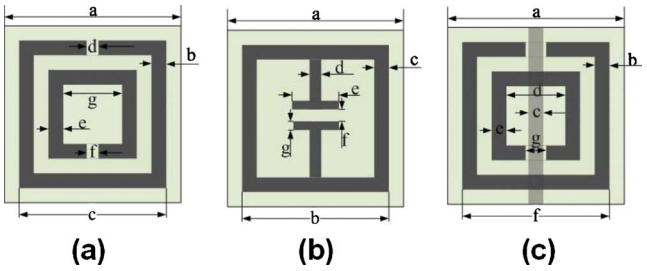

FIG. 2. (Color online) Three typical metamaterial structures. (a) The SRR structure. The substrate is Flame Resistant 4 (FR4), a type of material used for making a printed circuit board, whose relative permittivity is $\varepsilon=4.4+0.001i$ and thickness 0.25 mm. The dimensions in the figure are $a=2.5$ mm, $c=2.2$ mm, $g=1.1$ mm, $b=e=0.2$ mm, and $d=f=0.22$ mm. (b) The ELC structure. The substrate is still FR4 ($\varepsilon=4.4+0.001i$) with thickness 0.2026 mm. The dimensions are $a=3.333$ mm, $b=3$ mm, $c=d=g=f=0.2$ mm, and $e=1.4$ mm. (c) The SRR-wire structure. The substrate is FR4 ($\varepsilon=4.4+0.001i$) with thickness 0.25 mm. The SRR and wire are on different sides of the substrate. The dimensions are $a=2.5$ mm, $f=2.2$ mm, $b=e=0.2$ mm, $c=0.14$ mm, $d=1.1$ mm, and $g=0.3$ mm.

$$\bar{\varepsilon}_{\mathrm{ELC}} = \varepsilon_a[1 - Ff^2/(f^2 - f_0^2 + i\gamma f)], \tag{22}$$

and $\bar{\mu}_{\mathrm{ELC}}=\mu_a \sin(v)/v$. Here, f_0 is the electric resonant frequency. For the SRR with wire structure illustrated in Fig. 2(c), we have

$$\bar{\varepsilon}_{\text{SRR-wire}} = \varepsilon_a(1 - f_0^2/f^2), \tag{23}$$

$$\bar{\mu}_{\text{SRR-wire}} = \mu_a[1 - Ff^2/(f^2 - f_0^2 + i\gamma f)]. \tag{24}$$

Based on the ideal forms, we can now calculate the effective permittivity and permeability using Eqs. (19) and (20). Figure 3 compares the predicted parameters for the unit cell shown in Fig. 2(a) with those from direct simulation of a unit cell and a numerical S parameter retrieval. The S parameters are simulated using HFSS, a full-wave electromagnetic software whose accuracy has been verified earlier [10,14,17]. For the HFSS simulations, a single unit cell is simulated along the z direction, with periodic boundaries applied along the x and y directions. As can be seen from Fig. 3, there is remarkably good overall agreements between the analytic theory and the simulations, indicating that the approximation used for the wave impedance in Eq. (13) is appropriate.

The frequency regimes of various propagation modes can easily be identified from the phase advance shown in Fig. 3(c). Below the frequency of 9.6 GHz, the wave is propagating. From 9.6 to 10 GHz, the phase advance reaches 180° and hence the wave is in the resonant crystal band-gap regime. From 10 to 11.5 GHz, modes are evanescent. The resonant frequency of SRR occurs at 10 GHz. Above 11.5 GHz, all modes once again correspond to propagating modes. The numerical curve and theoretical curve have excellent agreement both qualitatively and quantitatively.

Based on the above analysis, it is easy to understand the behavior of theoretical prediction results for SRR. There is a huge jump in permeability and a dip for permittivity at 9.6 GHz, as shown in Figs. 3(a) and 3(b), because $\theta=180°$ at

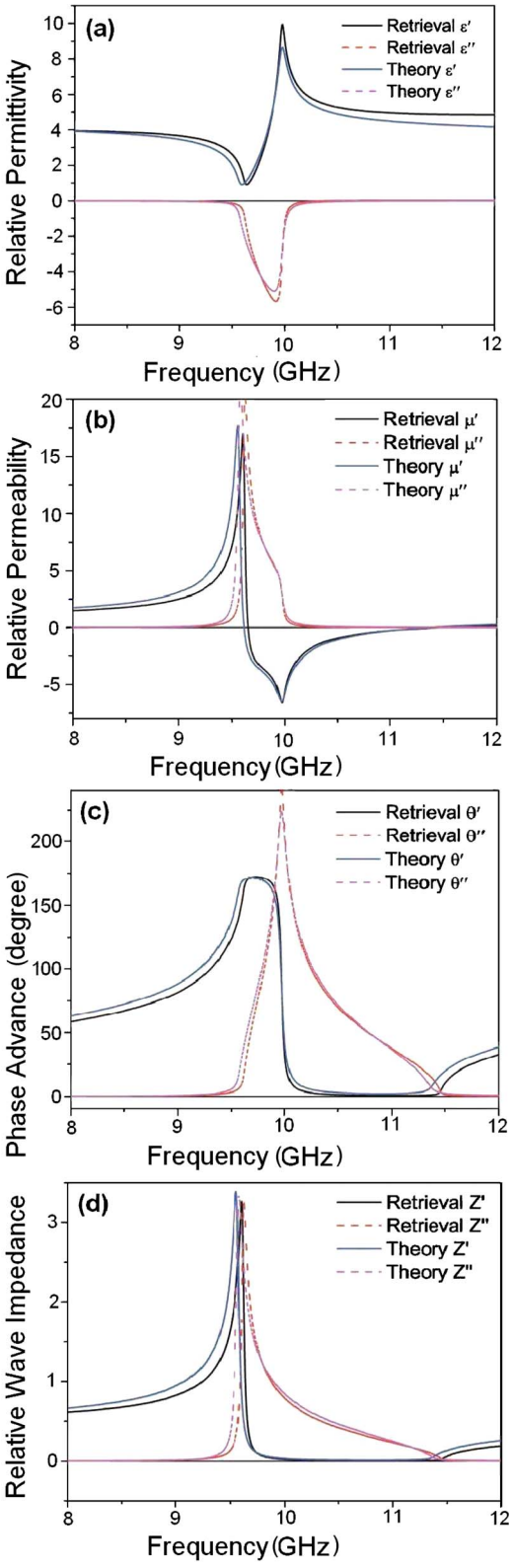

FIG. 3. (Color online) Comparison of theoretical prediction results and retrieval results from the parameters S for the SRR structure. The parameters using in the theoretical calculation are $f_0=9.975$ GHz, $\varepsilon_a=4.4\varepsilon_0$, $\mu_a=\mu_0$, $\gamma=5\times10^7$ Hz, $p=2.5$ mm, and $F=0.23$.

9.6 GHz acts as the interface of propagation modes and resonant crystal modes where the wave impedance becomes very large based on the general theory. Such a critical frequency for a resonant crystal band gap is sometimes inappropriately taken as the resonant frequency while the true value should be 10 GHz as in the previous analysis.

Next we consider the ELC structure shown in Fig. 2(b). In Ref. [16], experimental data for the *S* parameters were used to retrieve the effective permittivity and permeability. The retrieval results are illustrated in Fig. 3 in Ref. [16].

We can analyze the propagation modes of the ELC structure shown in Fig. 4(c) and the SRR-wire structure shown in Fig. 5(c). Clearly, all three propagation cases, propagation modes, pure plasma modes, and resonant crystal band-gap modes are obtained.

In the following discussions, we will emphasize three points: the resonant crystal band gap and its critical frequency adjacent to the propagation mode, the conjugate imaginary parts for the effective parameters or the *negative-loss* phenomenon, and the antiresonance for effective parameters.

First we study the resonant crystal band gap in a SRR, which is due to the strong resonance of a SRR and coupling among different SRRs. From the general theory, it is a magnetic resonant crystal band gap with right-handed dispersion (RHD) and a magnetic boundary. The average permittivity and permeability in such a band gap are both positive and the frequency is lower than the resonant frequency. Meanwhile, we also observe a similar resonant crystal band gap in the ELC structure shown in Fig. 2(b) from 10.8 to 12.3 GHz. It also has RHD but with an electric boundary. Unlike the resonant crystal band gap in a SRR, it results in a negative real part of the permittivity.

For the SRR-wire structure, we observe that the resonant crystal band gap occurs from 8.7 to 9.3 GHz, as shown in Fig. 5(c). Although we apply the magnetic boundary in such a structure, it is actually an electric resonant crystal band gap, whose real part of permittivity is negative. This is due to the left-handed dispersion (LHD) which gives a $-180°$ phase shift from each unit. The resonant frequency for a SRR in this structure is 8.8 GHz, lower than the crystal band-gap frequency. Comparing Figs. 3–5, the critical frequency for the resonant crystal band gap adjacent to the propagation mode is clearly observed. They are 9.6 GHz for the SRR, 10.9 GHz for the ELC, and 9.3 GHz for the SRR-wire structure. The spatial wave impedance becomes very large for SRR and SRR-wire structures but extremely small for the ELC structure, which corresponds to a dramatic jump and dip for the effective parameters.

Second, we emphasize the negative imaginary part for the effective parameters, which is referred as a negative-loss phenomenon. Based on the solution of the general theory, for lossless effective media, the effective permittivity and permeability may have conjugate imaginary parts (conjugate loss) within the resonant crystal regime due to the significant spatial wave impedance. For the propagation mode, the negative-loss phenomenon may occur in lossy media while it is relatively slight for low-loss media. We look back to Figs. 3–5. Within the resonant crystal band-gap regime for each structure, the conjugate imaginary parts of effective param-

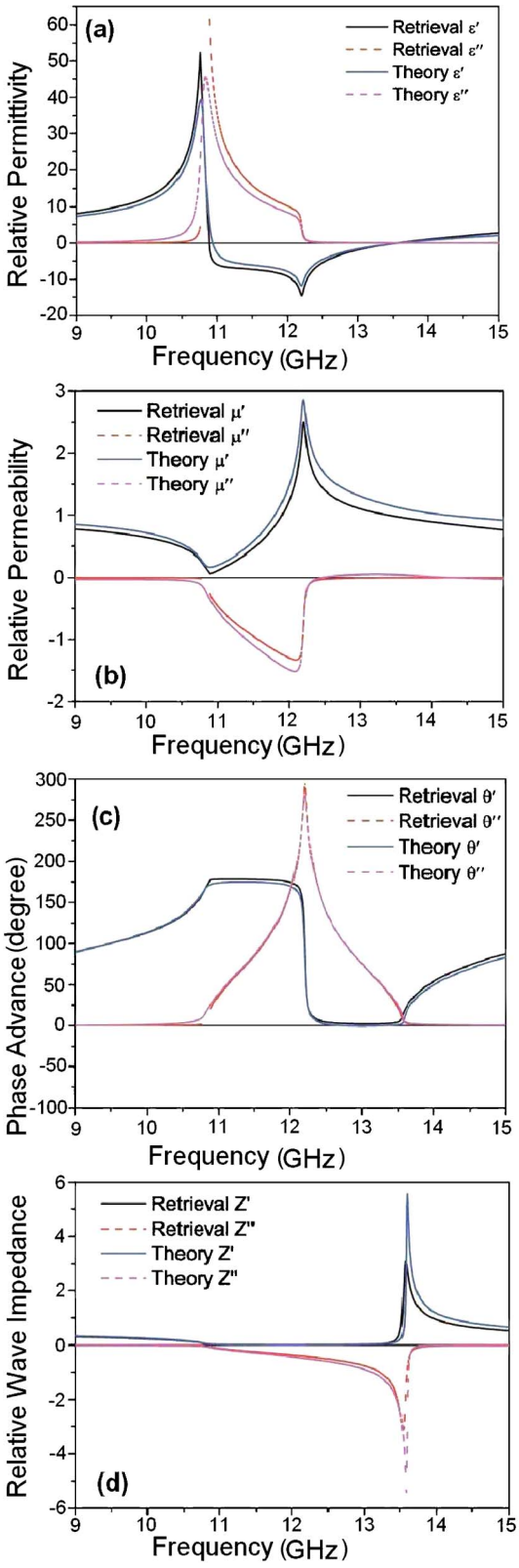

FIG. 4. (Color online) Comparison of theoretical prediction results and retrieval results from the scattering parameters *S* for the ELC structure. The parameters using in the theoretical calculation are $f_0=12.2$ GHz, $\varepsilon_a=4.2\varepsilon_0$, $\mu_a=\mu_0$, $\gamma=4\times10^7$ Hz, $p=3.333$ mm, and $F=0.19$.

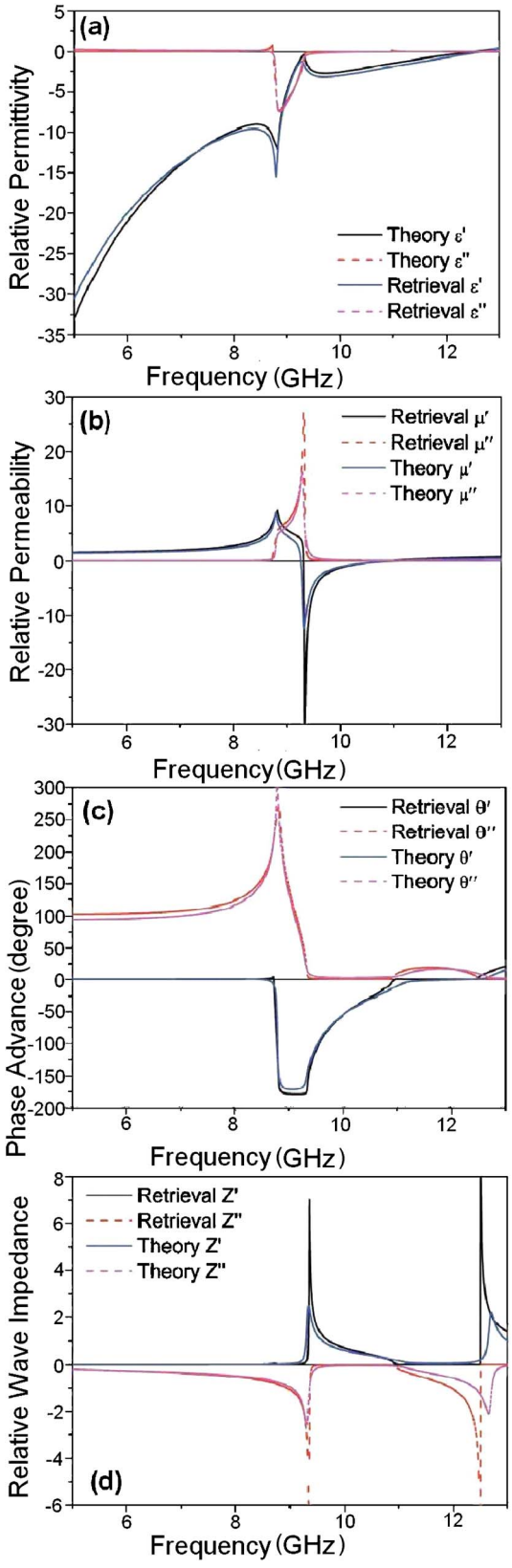

FIG. 5. (Color online) Comparison of theoretical prediction results and retrieval results from the scattering parameters S for the SRR-wire structure. The parameters using in the theoretical calculation are $f_0=8.8$ GHz, $\varepsilon_a=5\varepsilon_0$, $\mu_a=2\mu_0$, $\gamma=10^7$ Hz, $p=2.5$ mm, and $F=0.35$.

eters are well predicted in the theoretical result using Eqs. (19) and (20). For pure plasma modes, there is no conjugate-loss phenomenon predicted in the theory under the lossless situation. All these conclusions from the general theory can be supported by previous experimental observations [14,17].

The last issue is the antiresonant phenomenon in metamaterial structures. From Figs. 3–5, it is very clear that, when one of the effective parameters is resonant, the other one will have antiresonance spontaneously, no matter whether in the retrieval or the theoretical result. This phenomenon can be clearly explained by the general theory of effective media given in Eqs. (14) and (15). If p is not tending to 0, both effective parameters are determined not only by the average parameters but also by the phase advance θ. Therefore if one of the average parameters reaches a resonance, both the effective permittivity and permeability will be resonant; these are regarded as resonant and antiresonant phenomena [12].

VI. CONCLUSIONS

This paper provides a descriptive approach to and explanation of the electromagnetic behavior of metamaterials based on a general theory of effective media, from which the effective parameters are derived in terms of average permittivity and permeability. According to the derivations, we justify the validity of the effective medium theory for both homogeneous media and metamaterials. Meanwhile, three wave modes are categorized: the propagation mode, the pure plasma mode, and the crystal band-gap mode. We have compared and analyzed the behavior of SRR, ELC, and SRR-wire structures by theoretical predictions, using the general theory and numerical retrieval simulations. The analysis provides profound understanding of the resonant crystal band gap, the conjugate-loss phenomenon, and the antiresonant observation. Also the theoretical results match the retrieval results very well, giving a fitting formula for practical structures. This framework will significantly support the further analysis of more complicated periodic structures or even inhomogeneous particle structures. Also, the clear explanation and the accurate analytical formulations will give great guidance for synthesis and design of metamaterial structures.

ACKNOWLEDGMENTS

This work was supported in part by the National Basic Research Program (973) of China under Grant No. 2004CB719802, in part by the National Science Foundation of China under Grants No. 60671015, No. 60496317, and No. 60621002, and in part by the National Doctoral Foundation of China under Grant No. 20040286010. D.R.S. acknowledges support from the Air Force Office of Scientific Research through a Multiple University Research Initiative, Contract No. FA9550-06-1-0279.

[1] V. G. Veselago, Sov. Phys. Usp. **10**, 509 (1968).
[2] R. A. Shelby, D. R. Smith, and S. Schultz, Science **292**, 77 (2001).
[3] J. B. Pendry, Phys. Rev. Lett. **85**, 3966 (2000).
[4] T. J. Yen, W. J. Padilla, N. Fang, D. C. Vier, D. R. Smith, J. B. Pendry, D. N. Basov, and X. Zhang, Science **303**, 1494 (2004).
[5] J. B. Pendry, D. Schurig, and D. R. Smith, Science **312**, 1780 (2006).
[6] D. Schruig, J. J. Mock, B. J. Justice, S. A. Cummer, J. B. Pendry, A. F. Starr, and D. R. Smith, Science **314**, 977 (2006).
[7] D. R. Smith, W. J. Padilla, D. C. Vier, S. C. Nemat-Nasser, and S. Schultz, Phys. Rev. Lett. **84**, 4184 (2000).
[8] D. R. Smith and J. B. Pendry, J. Opt. Soc. Am. B **23**, 391 (2006).
[9] C. R. Simovski, e-print arXiv:cond-mat/0606622v1.
[10] D. R. Smith, D. C. Vier, Th. Koschny, and C. M. Soukoulis, Phys. Rev. E **71**, 036617 (2005).
[11] X. Chen, T. M. Grzegorczyk, B.-I. Wu, J. Pacheco, Jr., and J. A. Kong, Phys. Rev. E **70**, 016608 (2004).
[12] T. Koschny, P. Markos, D. R. Smith, and C. M. Soukoulis, Phys. Rev. E **68**, 065602(R) (2003).
[13] V. Varadan, Z. Sheng, S. Penumarthy, and S. Puligalla, Microwave Opt. Technol. Lett. **48**, No. 8 (2006).
[14] C. R. Simovski, P. A. Belov, and S. He, IEEE Trans. Antennas Propag. **51**, 2582 (2003).
[15] J. B. Pendry, A. J. Holden, and D. J. Robbins, IEEE Trans. Microwave Theory Tech. **47**, 2075 (1999).
[16] D. Schurig, J. J. Mock, and D. R. Smith, Appl. Phys. Lett. **88**, 041109 (2006).
[17] S. He, Z. Ruan, L. Chen, and J. Shen, Phys. Rev. B **70**, 115113 (2004).
[18] R. Liu, T. J. Cui, B. Zhao, X. Q. Lin, H. F. Ma, D. Huang, and D. R. Smith, Appl. Phys. Lett. **90**, 091912 (2007).
[19] R. Liu, B. Zhao, X. Q. Lin, Q. Cheng, and T. J. Cui, Phys. Rev. B **75**, 125118 (2007).
[20] R. Liu, B. Zhao, X. Q. Lin, and T. J. Cui, Appl. Phys. Lett. **89**, 221919 (2006).